



ORIGINAL ARTICLE

Effect of Direct yellow 50 removal from an aqueous solution using nano bentonite; adsorption isotherm, kinetic analysis and also thermodynamic behavior



Eman A. Alabbad

Department of Chemistry, College of Science, Imam Abdulrahman Bin Faisal University, P.O. Box 1982, Dammam 31441, Saudi Arabia

Received 20 June 2022; accepted 7 December 2022

Available online 12 December 2022

KEYWORDS

Nano bentonite;
Adsorption isotherm;
Kinetic studies;
Direct yellow 50;
Wastewater

Abstract The developing countries are suffering from the toxicity of different industrial effluents, especially dyes that contaminate water systems. This study successfully explained the preparation and characterization of nano bentonite to extract Direct Yellow Fifty (DY50). Direct Yellow 50 is an organic contaminant that may affect the quality of water. The characterization of prepared nanoparticles was done using Scanning electron microscopy (SEM), X-ray diffraction (XRD), and Fourier-transform infrared (FTIR). The impact of different operating conditions was studied using different pH, dose, temperature, contact time, and initial DY50 concentrations. The obtained results indicated that nano bentonite could adsorb about 94 % at initial concentrations of 40 mg/L, respectively. The optimum removal conditions were observed at an acidic pH (pH 3) using a sorbent material dosage of 0.05 g for 4 h at 30 °C. The adsorption isotherm, kinetic analysis, and thermodynamic behavior were studied using linear equation form, and the adjusted R^2 was compared to detect the preferred models. The adsorption behavior pseudo-second order kinetics, and fitted Langmuir isotherm model, respectively, showed the chemisorption interactions between adsorbed and sorbed molecules. Thermodynamic behavior indicated that the reaction was exothermic. Finally, this study strongly recommended using nano bentonite for DY50 removal from an aqueous solution.

© 2022 The Author. Published by Elsevier B.V. on behalf of King Saud University. This is an open access article under the CC BY-NC-ND license (<http://creativecommons.org/licenses/by-nc-nd/4.0/>).

1. Introduction

Water is an essential polar solvent all over the world (Mahmoud et al., 2019). So, it can carry out a broad range of inorganic and organic pollutants. The reuse of wastewater is the most critical solution to overcome water scarcity problems (Brown et al., 2009). Soluble organic pollutants are the most hazardous pollutants that all countries face, and they

E-mail address: ealabbad@iau.edu.sa

Peer review under responsibility of King Saud University.



Production and hosting by Elsevier

<https://doi.org/10.1016/j.arabjc.2022.104517>

1878-5352 © 2022 The Author. Published by Elsevier B.V. on behalf of King Saud University.

This is an open access article under the CC BY-NC-ND license (<http://creativecommons.org/licenses/by-nc-nd/4.0/>).

have difficulties getting rid of these contaminants in economic and fast ways (Cordell et al., 2009; Mahmoud et al., 2018). Different organic contaminants may affect water quality, such as colour, pesticides, carbon, nitrogen, and sulfur pollutants (Karam et al., 2020; Fan et al., 2009; Zhao et al., 2009; Ho et al., 2002). Color contaminants are one of the most common water and wastewater contaminants. Direct yellow 50 is one of these contaminants that may affect the quality of water (Wawrzkiwicz et al., 2021). The existence of colour in water and wastewater indicated a large number of organic carbons in the water or wastewater (Karam et al., 2020).

Many technologies were used to remove organic contaminants in different ways (Ho et al., 2002). The degradation and adsorption process is the most common treatment process used for organic contaminants removal (Mahmoud et al., 2020; Farahmandjou et al., 2015). Chemical coagulation, electrocoagulation, biodegradation, and filtration are also used for moderate organic and colour removal (Gheraout, 2009). Recently, nanotechnologies have been commonly used for organic removal from wastewater (Cincinelli et al., 2015).

Direct dye is azo dye, which is comparable to acid dyes. Primarily, dis-azo and tri-azo molecular game plans are commonly used due to direct dyes, besides a strong predominance of non-metallized natures to every shade independently (Alabbad, 2021). These sorts of dyes are usually used in numerous industries as essential colorants because of the simplicity of the products they provide, as well as the wide assortment of cost-effective and easily accessible items. In this manner, direct dyes have been widely utilized in various industries as of late, too (Derudi et al., 2007; Mo et al., 2008). Direct Yellow 50 is an example of a synthetic diazo dye made by Boruta-Zachem (Poland). Cellulosic fibers or their blends can be dyed using the water-soluble dye DY50, which is commonly used in the textile industry. DY50 has a molecular weight of 956.82 g/mol. Soluble in water and slightly soluble in ethanol. It is primarily used for cotton, viscose, and silk dyeing and printing, and it can directly print as well as discharge printing color. Electrochemical reactions can also be used to dye nylon, leather, paper, and aluminum (Wawrzkiwicz et al., 2020).

The fact that bentonite is an abundant raw material has many physical and chemical characteristics do not present in other minerals, such as its small particles being thixotropic, having a high swelling capacity, a porous interlayer, a high adsorption capacity, heat resistance, constant surface charge, and having a large ion exchange capacity (Khan et al., 2017; Tohdee et al., 2018). In addition, the weak nature of the bonds between the bentonite molecules makes it possible for water to easily pass between them, leading to their separation from one another and the bentonite's remarkable capacity to expand, which can reach eight times its initial size. From an economical point of view, bentonite is less expensive than other materials such as activated carbon, so it is used as a bio-sorbent for water treatment (De Camillis et al., 2016; Dehgani et al., 2020).

Nano bentonite has a strong ability to adsorb a broad range of wastewater and water contaminants due to its high surface and reactivity (Ahmed et al., 2015). Studied color removal from textile effluent using different techniques and indicated the ability of bentonite to adsorb basic dyes (Balaji et al., 2015). Mukhopadhyay studied bicarbonate and nitrate

removal from wastewater using nanoparticles (Iron Oxide and bentonite) and the obtained results indicated that Fe-exchanged nano bentonite can adsorb 29.33 mg/g after 120 min with significantly less than 0.05 g (Mukhopadhyay et al., 2019). Studied the efficient removal of cationic organic dye with the help of nanocomposite incorporated bentonite (Jana et al., 2019). Studied reactive dyes deletion from this aqueous solution using dirty bentonite and the obtained results indicated B-Mg (OH)₂ have strong ability to adsorb a wide range of dye concentration reached ~ 50 mg/g at acidic media after 3 h from contact time (Chinoune et al., 2016).

This study was directed toward using nano bentonite for the adsorption of waste materials that is easily prepared in many developing countries with the advantages of low cost and efficient adsorption of organic dyes and heavy metals from the aqueous media. This study attempts to examine and analyze the deletion of DY50 from an aqueous solution by nano bentonite. The synthesized nano bentonite was well characteristic for DY50 removal. The effect of various operating conditions was conducted to optimize the effective conditions. Finally, the adsorption isotherms, kinetic studies and thermodynamic behavior were designed to describe the reaction mechanism, equilibrium state, and spontaneous nature of the reaction.

2. Materials and methods

Practically, every substance was gotten from commercial sources and used without additional change. From Merck, the DY50 color was bought. The research works were carried out using an ultra violet-scanning spectrophotometer (which is UVD-2950 model) (LABOMED, Inc), the orbital shaker (steady shake, 757), as well as pH meter (Metrohm, 525A). The assortment of nano bentonite tests was carried out in Aramco Co., the Kingdom of Saudi Arabia.

The nano bentonite tests were distinguished through the X-ray diffraction method, which was suggested by the examination expert's dependent on their investigation conducted in (Önal et al., 2007). The cation exchange capacity (CEC) calculation was also based on (Kelessidis et al., 2007) techniques.

2.1. Preparation and characterization of nano bentonite

Nano bentonite was obtained as a gift from Aramco Co., Kingdom of Saudi Arabia as mentioned previously, and the method of preparation using flotation and sedimentation techniques was provided in supplementary materials. Using IRAFFINTT-2 as Fourier Transform an Infrared gear, the example for spectra were also described between 400 and 4000 cm⁻¹. The powdered sample was studied by XRD using the SHIMADZU (XRD-7000), with Cu as the target, (40 kilo Volt), 30 mega Ampere, scan range five to eighty degrees, and scan speed of 2 degrees per minute.

Besides, when performing absorption tests, a SEM "FEI, Inspect S50, Czech Republic" has been applied to capture micrographs at different amplifications at a speed up voltage of 20 kV. For analysis of pore size and surface area, a Brunauer-Emmett-Teller (BET) analyzer for surface area was used, "NOVA 1200 e", with N₂ as the analysis gas, analysis time of 130.5 min, and shower temperature (273 K).

2.2. DY50 solution preparation

With no extra purification, the chemical formula of “DY50 powder” ($C_{35}H_{24}N_6Na_4O_{13}S_4$) was used as a standard solution (anionic) that was set up by dissolving [DY50 powder] within distilled water. DY50’s constitution is depicted in the diagram below in Fig. 1. Sequential dilution was used to prepare the concentrations of the dye (1, 3, 5, 7, 10, 15, 20, and 30 ppm). At a $[\lambda = 412 \text{ nm}]$ wavelength, these concentrations were used to build a calibration curve. Following that, the concentrations of vague dye solutions were detected based on the calibration curve.

2.3. DY50 dye adsorption onto nano bentonite

The dye removal was studied using the batch equilibrium reaction. At first, a 100 mL DY50 solution was placed in a 500 mL bottle and held for 45 min at 30 °C with a 0.05 g sorbent. Using 1.0 mol HCl and 1.0 mol NaOH the pH was adjusted from 2.0 to 10.0.

To examine the effect of this contact time at the dye evacuation, a similar cycle was used with different cycles 5, 10, 20, 30, 60, 120, 240, 480, and 1440 min. A similar experiment was also conducted at different DY50 color concentrations (25.0 mL) with 20.00, 40.00, 60.00, 80.00, and also 100 mg/L

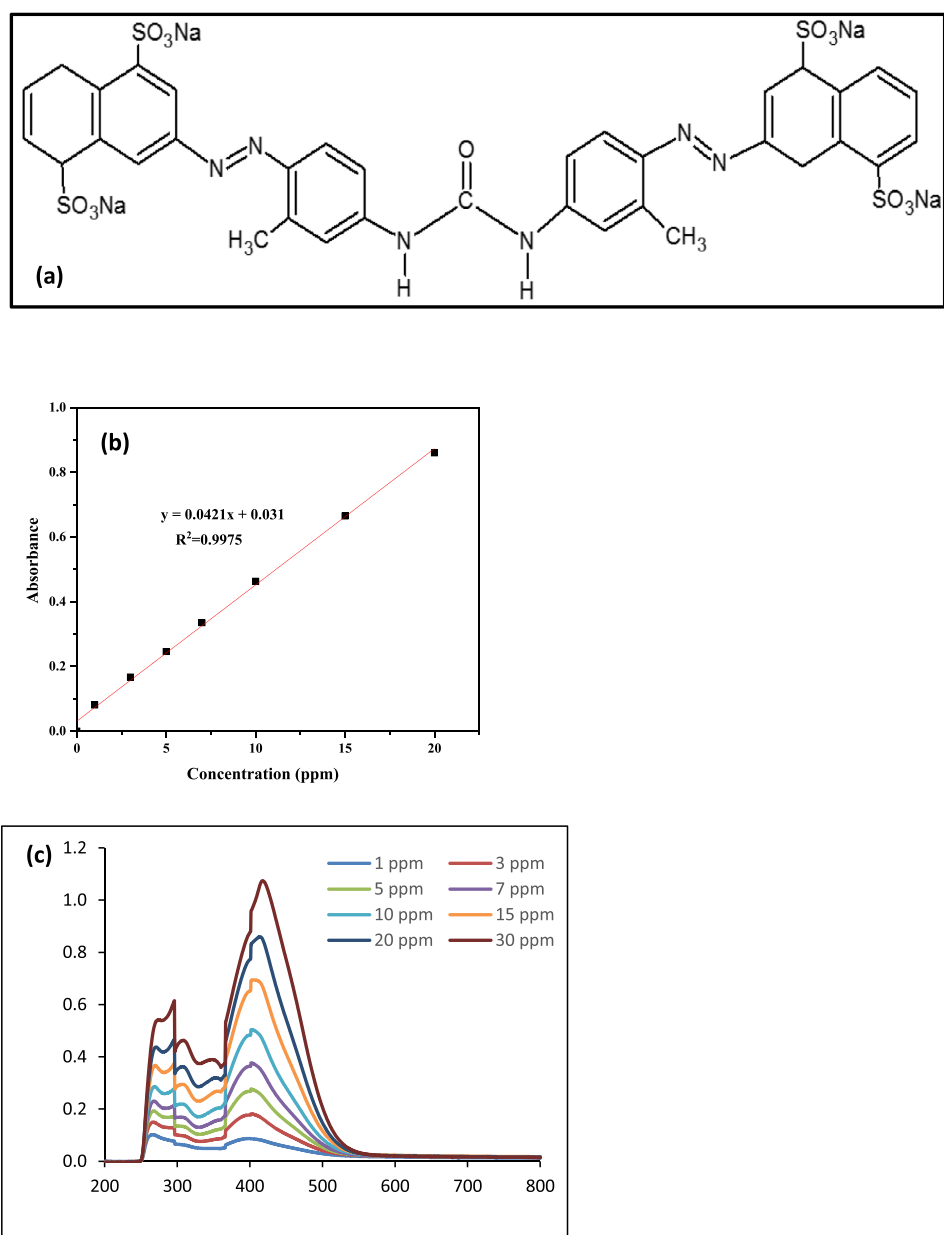


Fig. 1 (a) Direct Yellow 50 Structure, (b) Direct Yellow 50 calibration curve, and (c) Direct Yellow scanning with maximum absorbance, $\lambda_{max} = 412 \text{ nm}$.

and temperatures 20, 30, 40, 50, 60, and 70 °C. The dye adsorbent of several weights 0.01, 0.02, 0.05, 0.1, 0.2, and 0.3 g was also used to investigate the effect of the nano bentonite quantity. As a result, all samples were filtered, and the residual DY50 quantity has been calculated using ultra-violet visible spectroscopy “ λ 300 to 800 nm”. The information on absorbance was collected at the maximum wavelength [λ].

At equilibrium state, DY50 quantity of dye adsorbed “ Q_e ”, was assessed through Eq. (1):

$$Q_e(\text{mg/g}) = \frac{(C_0 - C_e)/v}{m} \quad (1)$$

Where Q_e (mg/g) DY50 absorbed/g sorbent, while v represents a volume of DY50 solution L, $[C_0]$ is an initial DY50 concentrations, m represents weight of nano bentonite in grams, and C_e is DY50 equilibrium concentrations (mg/L). The quantity of DY50 filtered and extracted at different intervals during the adsorption study was calculated using Eq. (2): During the adsorption analysis, the DY50 quantity that were filtered and removed at various intervals has been valued by Eq. (2):

$$Q_t = \frac{(C_0 - C_t)V}{W} \quad (2)$$

Where C_t denotes the concentration of DY50 in liquid (mg/L) at various times (t).

3. Results and discussion

3.1. Characterization of nano bentonite samples:

Nano bentonite is another class of microporous materials with great surface areas that have been widely concentrated as remarkable material in catalyst applications and adsorbents. The portrayal of bentonite was done utilizing an Infrared (IR) spectrophotometer, Transmission Electron Microscopy which is also known as TEM and X-ray diffraction (XRD), instruments. The CEC investigates by balancing the negative charges on the surface with positive charges in the form of exchanged sodium cations. The CEC of nano bentonite is 35.67 meq/100 mL and it is similar previously research’s (Kelessidis et al., 2007).

3.2. BET analysis of nano bentonite samples

BET test illuminates the interaction regarding gas molecules’ adsorption onto a flat substrate on a physical scale, which is the basis for the estimation of specific surface area (SSA) of several sample ingredients. Also, the N_2 adsorption-desorption isotherms were used to determine the size of pores and the SSA of the nano bentonite samples.

As a result, samples were analyzed in Fig. 2 for quantifying the adsorption rate, which also revealed the desorption rate for nano bentonite. Those adsorption-desorption rates were used to define the samples surfaces and pore sizes where the measurements were taken. Therefore, the calculated SSA of the samples was to be (79.07 m^2/g), the average pore size was (4.982 nm) and the pore size was (0.1970 cm^3/g). The mesoporous size was ($d > 2$ nm); along these lines, the nano bentonite in the present analysis might be like a mesoporous substance (Duman et al., 2009).

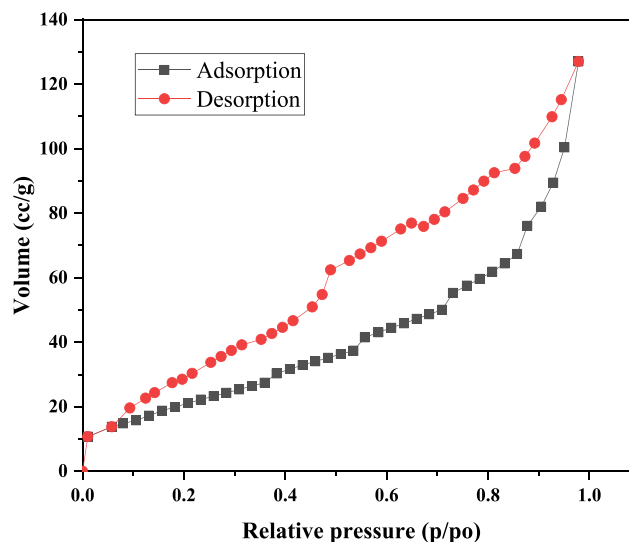


Fig. 2 BET-BJH analysis of nano bentonite before and after adsorption.

3.3. FTIR analysis of nano bentonite samples

The nano bentonite experiments used FTIR to measure and analyze the sample’s structure by analyzing the initiated reactions within the nano bentonite pores. In order to obtain structural data for the nano bentonite tests, the vibrational frequencies that were hence enrolled in the nano bentonite lattice were investigated (Van olphen, 1977).

The FTIR results of the prepared samples are shown in Fig. 3, which revealed an O—H vibration band between 3600 and 3300 cm^{-1} . A sharp absorption beam shows up at around 1637 cm^{-1} in the absorption spectrum of nano bentonite because of the bowing vibrations of the water molecules. Additionally, Si—O—Si stretching vibration band (SVB) at 1035 cm^{-1} , Si—O—Si bending vibration band somewhere in the range of 526 and 471 cm^{-1} . what’s more, Al—O—Si SVB at 800 cm^{-1} .

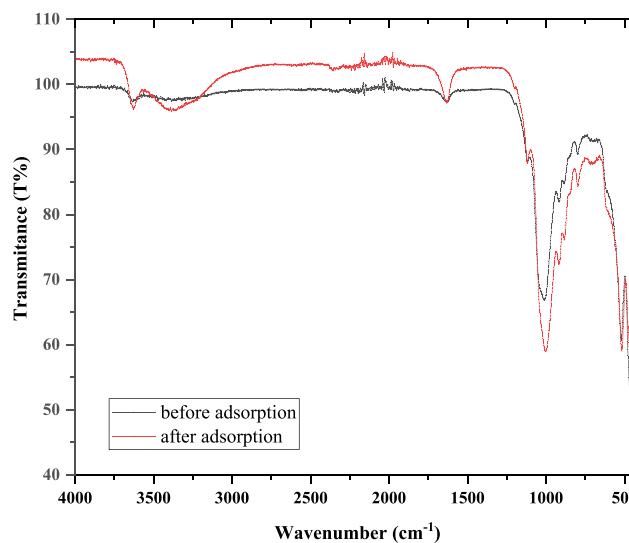


Fig. 3 The Infrared spectra FTIR of nano bentonite before and after DY 50 adsorption.

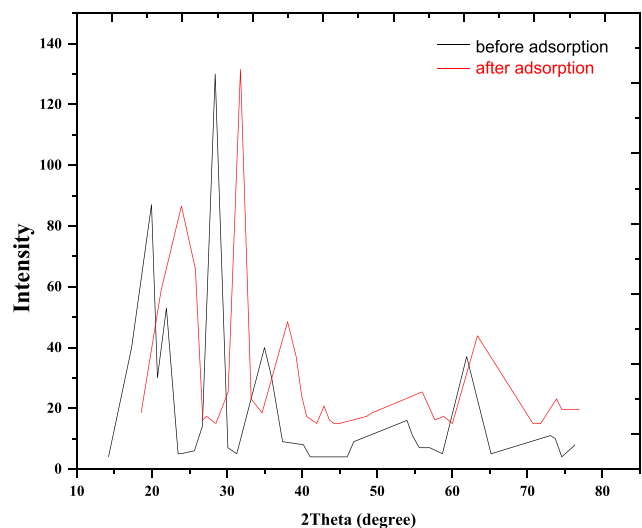


Fig. 4 The measured qualitative XRD mineralogical composition of nano bentonite before and after DY50 adsorption.

The acquired FTIR results concur with the past nano bentonite portrayal considers. The absorption spectrum of the samples additionally shows the presence of spectral lines for the bending modes and the deformation of the Al—Al—OH and Al—Fe—OH at $826, 908 \text{ cm}^{-1}$ individually (Darvishi et al., 2011; Cozzolino et al., 2006).

3.3.1. XRD analysis of nano bentonite samples

The XRD was an exceptionally proficient analysis technique used to detect the crystalline phases of tests, providing knowledge on the dimensions of the unit cell as well as related molecular characteristics. The XRD test for nano bentonite that appeared in Fig. 4 exhibits the presence of clear lines in a crystalline state (Van olphen 1977). The XRD diffraction model is also used for distinguishing between bentonites by knowing their interlayer spacing to lay it out each clay has a particular worth from the d-dimension. The XRD pattern of the nano bentonite test additionally showed reflection intensity, with diffraction peaks at 2θ is 6.70° for nano bentonite and the interplanar distance when $n = 1$ is 13.18 \AA . This is because

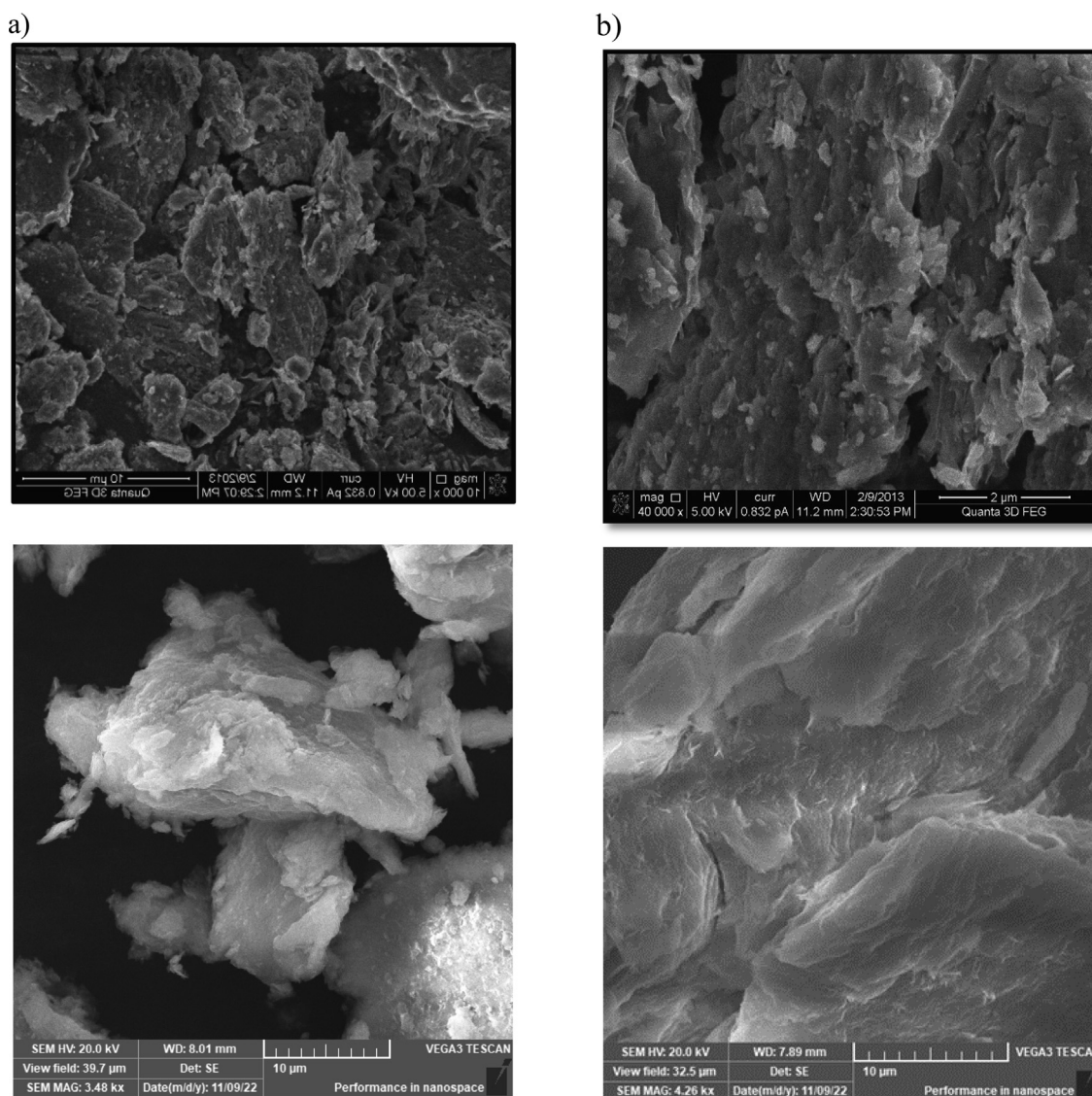


Fig. 5 SEM picture of nano bentonite (a) prior to adsorption and (b) following adsorption.

of the swelling and the hardness of the water while showing the water during the adsorption process (Önal et al., 2007).

3.3.2. SEM and EDX characterization of nano bentonite samples

The SEM creates microstructural images with a variety of samples by revealing them to different frequencies and wavelengths of electron beams, depending on the specifications and the content of the example. When conducting nano bentonite adsorption experiments, SEM was also applied to inspect the surface morphology. Micrographs at varying magnifications were captured using a SEM with a [20 kV] speed up voltage. Then, the pictures were utilized to show the nano bentonite topology and morphology on the outside. The nano bentonite surface test had either a harsh or mesoporous/miniature morphology with different cracks, as shown in SEM (Fig. 5(a) and (b)), suggesting a greater surface area that is useful for material adsorption.

The morphology of the nano bentonite test, after adsorption, was slightly transformed from a disjointed, cracked, and rough structure to the smoother and more conjoined strong face with fewer cracks, demonstrating porous areas filled with the adsorbed materials (Darvishi et al., 2011; Pacula et al., 2006).

The EDX of a nano bentonite particle is shown in Fig. 6. The results show that it contains the basic elements for the composition of montmorillonite, which are mainly O, Al, Si and a small percentage of Fe, Mg. The results also confirm the presence of Na, meaning that the clay used is Na-Montmorillonite. The figure also shows the analysis by micro-

electronic examination, where the electromagnetic orientation of a beam of electrons occurs, making it possible to examine a very small part of the sample within $1 \mu\text{m}^3$, where the primary X-rays from the sample are measured, which It is used in this case as an anode, and using a special optical microscope, the composition of the sample can be determined. It appears from the figure that there is more than one component in the structure of the nano bentonite as seen in Table 1, which determines the percentage of elements in the nanoparticles by EDS.

3.4. The effect of pH on DY50 removal

The impact of pH with rate of adsorption, among [3.00 to 10.0] is explained in Fig. 7. The highest DY50 removal (96.7 %) was documented at pH [3.0] with a nano bentonite weight of [0.05 g], then a decrease of pH value at pH 5 and 8 to (93.9 %). It is obvious that DY50 adsorption on the nano bentonite surface is essentially affected by a surface charge on the adsorbent. Nano bentonite has point of zero charge (pHPzc) value at pH 6.0 in Fig. 8. The (pHPzc) value for nano bentonite between pH 5 to 8 and it is corresponding to research values (Bourg et al., 2007).

When the pH of the adsorbent decreases, its charge becomes more positive, and adsorbs more anionic species. In an aqueous solution, DY50 dissociates to produce the anion form which in acidic condition the removal is well accomplished because of this electrostatic attraction among the protonated adsorbent surface as well as the negative sulfonated

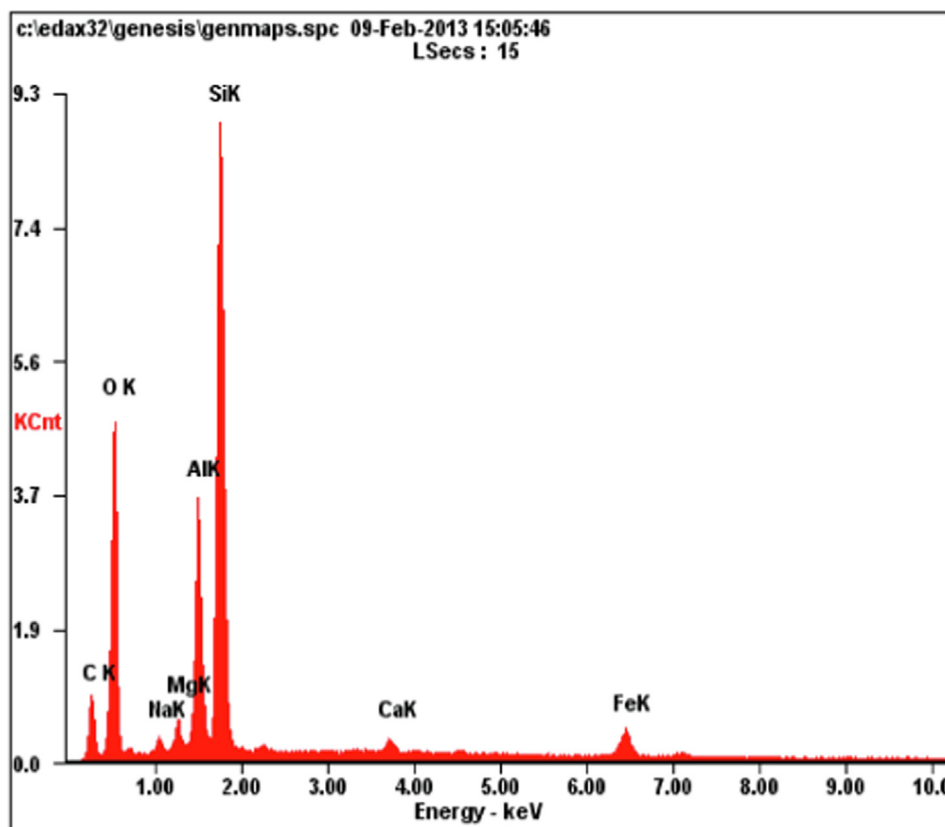


Fig. 6 EDS analysis of nano bentonite.

Table 1 EDS for nano bentonite.

Element	Wt%	At%
CK	22.11	32.08
OK	42.44	46.22
NaK	00.90	00.68
MgK	01.25	00.89
AlK	09.07	05.86
SiK	21.49	13.33
FeK	02.21	00.69
CaK	00.54	00.24

groups of the dissociated dye molecules. With increasing pH, the measure of adsorbed DY50 through nano bentonite was found to be decreased. Besides that, at high pH values, removal is decreased due to the competition with hydroxyl ions

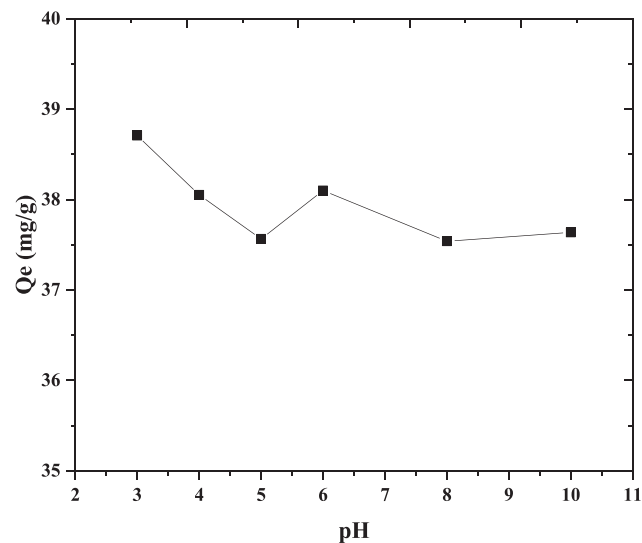
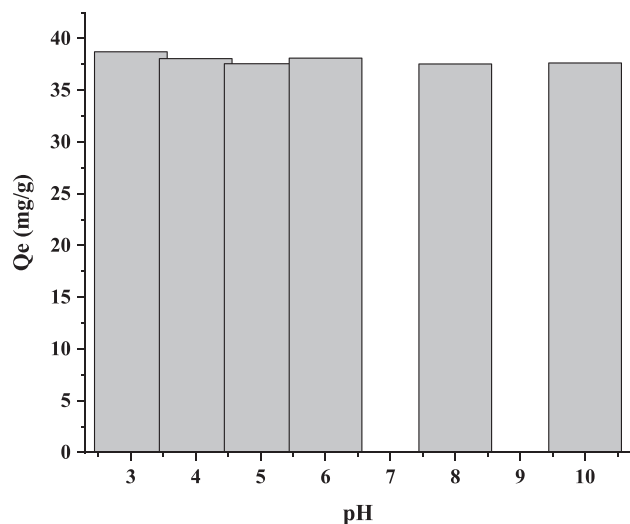


Fig. 7 Effect of pH on DY50 removal by nano bentonite “DY50 (40 ppm), T (30 °C), W (0.05 g) and t (4 h)”.

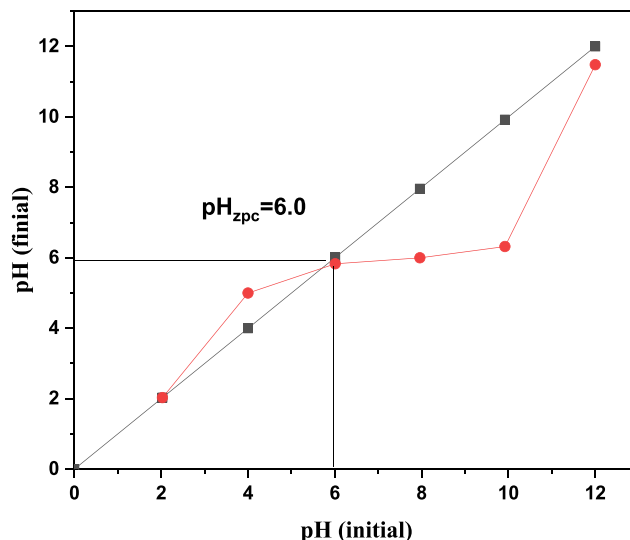


Fig. 8 Zero charge analysis of the nano bentonite adsorbent.

that restricted the oncoming of dye anions (Khraisheh et al., 2004).

3.5. Isothermal analysis and the influence of DY50 concentration

At temperature 30° C and pH 3.0, the DY50 concentration influence on the adsorption interaction is shown in Fig. 9. The primary DY50 concentration had a direct correlation to the adsorptive ability of the dye onto nano bentonite, as shown in the figure. As a result, it was recognized that dye adsorptive strength can be adjusted via controlling the underlying quantity of dye. Following that, the DY50 adsorption onto nano bentonite was examined using Temkin, Langmuir, and Freundlich isotherm recreations with a straightened plot. The present study showed isothermal adsorption, which is the

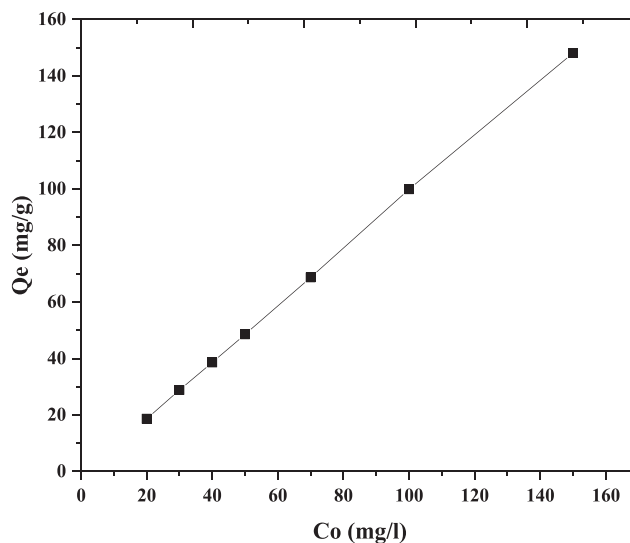


Fig. 9 Impact of initial DY50 concentration on the equilibrium adsorption capacity of nano bentonite [W = 0.05 g, pH = 3, T = 30 °C, t = 4 h].

Table 2 Assessment for the elimination data of DY50 in accord to the Temkin isotherms, Langmuir and Freundlich.

Freundlich isotherm			Langmuir isotherm				Temkin isotherm		
K_F (mg/g)(mg/L) ^{1/n}	n	R ²	Q_0 (mg/g)	K_L (L/mg)	R_L	R ²	B (J/mol)	A (L/g)	R ²
43.7219	1.3614	0.9779	250	0.2259	0.04237	0.9886	46.553	3.0926	0.9771

Table 3 Comparison for maximum adsorption capacities for removing of DY50 by the use of various adsorbent substances.

Sorbents	Q ₀ (mg. g ⁻¹)	Ref.
Nanobentonite	250	This study.
Activated carbons from surplus sewage sludge	188	(Martin et al., 2003)
Activated Algerian clay	175.74	(Elhadi et al., 2020)
Zeolite	83.33	(Alabbad et al., 2021)
Natural sugarcane stalks powder	20.96	(El-Sayed et al., 2013)
Silica	3.03	(Koyuncu et al., 2009)

distribution strategy for adsorbed molecules in an equilibrium state between the liquid and solid phases.

The Langmuir model of isotherm has been expressed via Eq. (3):

$$C_e/Q_e = 1/(Q_0 K_L) + C_e/Q_0 \quad (3)$$

The Langmuir model of adsorption constants were [Q₀] is associated to this adsorption capacity (given in mg/g) and [K_L] is associated to the adsorption energy (L/mg).

Moreover, the Langmuir isotherm model's basic properties were expressed using R_L, dimensional coefficient separation factor, which has been defined as Eq. (4):

$$R_L = \frac{1}{1 + K_L C_e} \quad (4)$$

The isotherm can be determined according to the R_L benefit, with the isotherm being linear in case that R_L = 1, unfavorable in case that R_L > 1, and moreover (0 < R_L < 1) was favorable or here (R_L = 0) being irreversible.

Eq. (5) expresses a Freundlich model that was satisfactory at little concentrations and heterogeneous surfaces:

Table 4 Effect of adsorption dosage of nano bentonite on DY50 at pH 3.

W (g)	Q _e (mg/g)	Removal (%)
0.01	181.49	90.74
0.02	94.58	94.58
0.05	38.39	95.97
0.1	19.31	96.58
0.2	9.84	98.41
0.3	6.61	99.20

$$\log q_e = \log K_f + \frac{1}{n} \log C_e \quad (5)$$

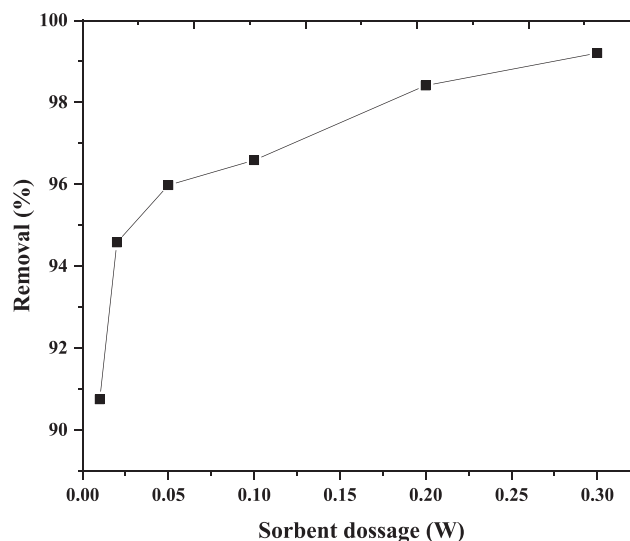
In the Freundlich adsorption model, the K_F constant refers to an adsorption capacity (mg/g) and also n constant refers to an adsorption intensity. All necessary parameters will be detected using the intercepts and slope of a linear plotted between log C_e and log q_e.

A Temkin model will be used to depict the effect of back-handed desorption / adsorption reactions at adsorption temperature. Temkin model was based on the way in which adsorption reduces the heat of adsorption of all molecules linearly. Eq. (6) addresses isotherm that results from the Temkin model:

$$q_e = \frac{RT}{b} \ln AC_e \quad (6)$$

Where b equal to RT/b equal to (RT/ΔE) Q₀, R was a general gas constant with [8.314 J/mol K] value, T equal to Kelvin temperature, also Temkin equilibrium constant (L/mg) equal to A "maximum binding energy", variety adsorption energy (Joule/mol), and, ΔE = (- ΔH). This notation used for Temkin equilibrium is given by a letter A, also an adsorption (maximum) potential is denoted by the letter Q₀ (Kundu et al., 2006). Table 2 shows B and A from a slope, as well as a plot q_e capture against plot C_e.

The Freundlich isotherm's constant K_F which reflects the capacity of the adsorption was nearly (43.7219 mg/g). In addition, the R² for an isotherm framed in the Freundlich, Lang-

**Fig. 10** Effect of nano bentonite dose on DY50 removal "DY50 (40 ppm), pH (3), T (30° C), t(4 h)".

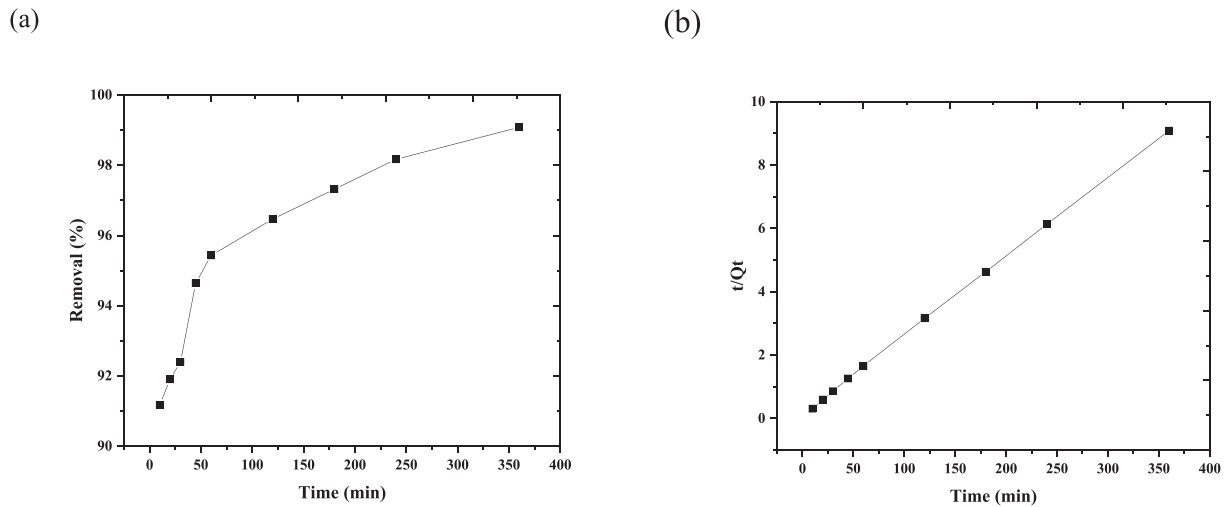


Fig. 11 (a) The contact time impact on removal of DY50 by nano bentonite “DY50 (40 ppm), T(30° C), pH(3), W(0.05 g)”, (b) Pseudo 2nd -order kinetic model.

Table 5 Kinetic parameters for the pseudo 1st and 2nd order.

$(Q_e)_{Exp}$ (mg/g)	Pseudo 1st order			Pseudo 2nd order		
	$(Q_e)_{Cal}$ (mg/g)	K_1 (min^{-1})	R_1^2	$(Q_e)_{Cal}$ (mg/g)	K_2 ($g\ mg^{-1}\ min^{-1}$)	R_2^2
39.63	3.1174	0.0089	0.9693	39.37	0.0147	0.9999

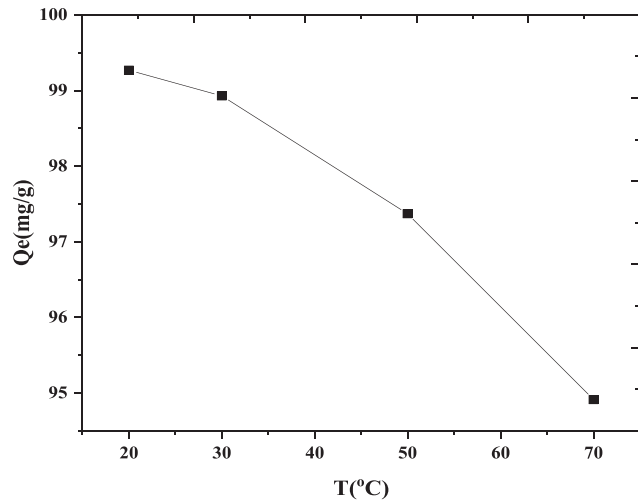


Fig. 12 Effect of the temperature on DY50 removal by nano bentonite “DY50 (40 ppm), pH(3), W (0.05 g), t (4 h)”.

muir, and Temkin models, respectively, was 0.9779, 0.9886 and 0.9771. Additionally, the maximum evacuation potential Q_0 was estimated to be 250 mg/g, and (K_L) adsorption coefficient was (0.2259 L /mg).

It is clear that the favorable model was shown to be the Langmuir isotherm. It is most suitable the equilibrium data (Afshin et al., 2018).

Table 3 shows this sorption capacity of nano bentonite for direct yellow removal and numerous sorbent materials. The

capacity of nano bentonite to remove DY is nearly comparable or even superior to that of other implemented sorbents, indicating that the sorbents used in this study have amazing ability to treat the waste effluents.

3.6. The nano bentonite dose impact

The nano bentonite dose is a significant parameter for adsorption. It affects the adsorption capacity of adsorbents. The impact of the nano bentonite dose of DY50 removal at the concentration of 40 mg /liter was studied and illustrated in Table 4 and Fig. 10. The dose varied from 90.7 to 99.2 %, with the dose being increased from 0.01 g to 0.30 g, respectively. The DY50 adsorption increases with increasing dose of nano bentonite. This could be because of the improved availability of these adsorption sites resultant from a rise in the dose and agglomeration of an adsorbent material, and saturation is due to this occupation of the active sites (Khodaer et al., 2015; Sadaf et al., 2015; Diouri et al., 2019).

3.7. The effect of sorption period and kinetic analysis

This adsorption time, whose kinetic analysis was also given in Fig. 11, is another factor that influences the adsorption interaction. The got results demonstrated that the removal proficiency expanded with time and the minimum viable time was 45 min with a removal percentage of 94.6 %. The pseudo 1st and 2nd kinetic orders (Eq. (7) and Eq. (8)), respectively, were used to prepare the kinetic information. The dye adsorption on several sorbents may be more accurately depicted by models of

Table 6 Thermodynamic parameters for DY50 removal on nano bentonite at various temperatures.

ΔH	ΔS	ΔG (KJ/mol)			
(KJ/mol)	(J/mol K ⁻¹)	$T = 20$ °C	$T = 30$ °C	$T = 50$ °C	$T = 70$ °C
-33.7733	-74.19	-11.9658	-11.4027	-9.7033	-8.3486

pseudo 1st order and 2nd kinetic order (Alabbad et al., 2019; Alakhras et al., 2019).

Pseudo 1st order:

$$\ln(Q_e - Q_t) = \ln Q_e - k_1 t \quad (7)$$

Pseudo 2nd order:

$$\frac{t}{Q_t} = \frac{1}{k_2 Q_e^2} + \frac{t}{Q_e} \quad (8)$$

The equilibrium was achieved after 180 min at 97.19 mg/L DY50 dye concentrations, mirroring the regulation of excess active sites at a adsorbent surface.

As given at Table 5, (R_2^2) of a pseudo 2nd order (0.9999) noticeably was larger than (R_1^2) of pseudo 1st order (0.9693).

Before all else, the removal percentages surpass 90 % because of the great surface area and reactivity of nano bentonite. Khodaer examined DY50 evacuation utilizing natural clay and organoclay, and the acquired results showed that the maximum time was 40 min in the wake of utilizing bentonite and changed bentonite as sorbent materials (Khodaer et al., 2015).

In the present study, this pseudo 2nd order kinetics model was dominant, and an immediate adsorption rate regulation in the complete kinetics adsorption was observed. (Wu et al., 2009) performed an investigation that confirmed this.

3.8. The effect of thermodynamic and temperature

DY50 adsorption on nano bentonite was carried out at temperatures of 20, 30, 50, and 70 °C, with the other parameters remained constant at their ideal values in Fig. 12. As the temperature rises from 20 °C to 70 °C, the adsorption capacity falls from 99.2 to 94.9 %. This is due to either the adsorbent's dynamic binding destinations being damaged or the growing dye's tendency to desorb from an interface near the solution. These results demonstrate exothermic existence of an adsorption cycle.

The thermodynamic capacities were evaluated in the dye-adsorbent structures to determine if the adsorptive cycle is exothermic or endothermic. Table 6 shows the progressions in enthalpy (ΔH), free energy (ΔG) and entropy (ΔS), and as parameters for investigation of thermodynamic character. All ΔG values were found to be negative, indicating that DY50 adsorption onto nano bentonite is exothermic.

The entropy change was negative, indicating that the framework's entropy decreased during adsorption. (Sheshdeh et al., 2014). The mechanism of adsorption has been discovered using these parameters (Konicki et al., 2017; Aid et al., 2018).

4. Conclusions

According to the findings of the DY50 removal of color from water using nano bentonite, there was an important impact

that the initial DY50 concentration, contact time, temperature, pH, and adsorbent mass all had on the DY50 adsorption on nano bentonite. The prepared nano bentonite was characterized using SEM, XRD, and FTIR analysis. The obtained data showed that nano bentonite could adsorb about 94 % at initial concentrations of 40 mg/L, respectively. The optimum removal conditions were observed at an acidic pH (pH 3) using a sorbent material dosage of 0.05 g for 4 h at 30 °C. The isothermal model confirmed that DY50 color adsorption on the nano bentonite surface is favorable. Using a chemisorption cycle that was a pseudo-second-order kinetic model, the DY50 adsorption ability was high and well regulated. Dye expulsion interacts in a random and exothermic manner. The Langmuir isotherm was found to be the most suitable model among the three models described.

5. Data availability statement

Data sharing is not applicable to this article as no data sets were generated during the present study.

Declaration of Competing Interest

The authors declare that they have no known competing financial interests or personal relationships that could have appeared to influence the work reported in this paper.

Acknowledgments

I give thanks to everyone who offered me support and encouragement throughout the study.

References

- Afshin, S., Mokhtari, S.A., Vosoughi, M., Sadeghi, H., Rashtbari, Y., 2018. Data of adsorption of Basic Blue 41 dye from aqueous solutions by activated carbon prepared from filamentous algae. *Data Brief* 21, 1008–1013. <https://doi.org/10.1016/j.dib.2018.10.023>.
- Ahmed, M.B., Zhou, J.L., Ngo, H.H., Guo, W., 2015. Adsorptive removal of antibiotics from water and wastewater: progress and challenges. *Sci. Total Environ.* 532, 112–126. <https://doi.org/10.1016/j.scitotenv.2015.05.130>.
- Aid, A., Amokrane, S., Nibou, D., Mekatel, E., Trari, M., Hulea, V., 2018. Modeling biosorption of Cr(VI) onto *Ulva compressa* L. from aqueous solutions. *Water Sci. Technol.* 77 (1), 60–69. <https://doi.org/10.2166/wst.2017.509>.
- Alabbad, E.A., 2019. Estimation the sorption capacity of chemically modified chitosan toward cadmium ion in wastewater effluents. *Orient. J. Chem.* 35 (2), 757–765. <https://doi.org/10.13005/ojc/350236>.
- Alabbad, E., 2021. Efficacy assessment of natural zeolite containing wastewater on the adsorption behaviour of Direct Yellow 50 from; equilibrium, kinetics and thermodynamic studies. *Arab. J. Chem.* 14, 103041.

- Alakhras, F., 2019. Kinetics and diffusion analysis for the removal of cadmium ion from aqueous solutions using chitosan-iso-vanillin sorbent. *Russ. J. Phys. Chem. A* 93, 2628–2634. <https://doi.org/10.1134/S0036024419130041>.
- Balaji, P., Vignesh, B., Sowmiya, M., Meena, M., Lokesh, L., 2015. Removal of colour from textile effluent using natural adsorbent (Calotropis Gingantea). *Int. J. Innovations Eng. Technol.* 5 (4), 265–272.
- Bourg, I.C., Sposito, G., Bourg, A.C.M.J., 2007. Modeling the acid-base surface chemistry of montmorillonite. *J. Colloidal Interface Sci.* 312, 297–310. <https://doi.org/10.1016/j.jcis.2007.03.062>.
- Brown, R.R., Keath, N., Wong, T.H.F., 2009. Urban water management in cities: historical, current and future regimes. *Water Sci. Technol.* 59 (5), 847–855. <https://doi.org/10.2166/wst.2009.029>.
- Chinoune, K., Bentaleb, K., Bouberka, Z., Nadim, A., Maschke, U., 2016. Adsorption of reactive dyes from aqueous solution by dirty bentonite. *Appl. Clay Sci.* 123, 64–75. <https://doi.org/10.1016/j.clay.2016.01.006>.
- Cincinelli, A., Martellini, T., Coppini, E., Fibbi, D., Katsoyiannis, A., 2015. Nanotechnologies for removal of pharmaceuticals and personal care products from water and wastewater. a review. *J. Nanosci. Nanotechnol.* 15, 3333–3347. <https://doi.org/10.1166/jnn.2015.10036>.
- Cordell, D., Drangert, J.-O., White, S., 2009. The story of phosphorus: global food security and food for thought. *Glob. Environ. Chang.* 19, 292–305. <https://doi.org/10.1016/j.gloenvcha.2008.10.009>.
- Cozzolino, D., Moron, A., 2006. Potential of near-infrared reflectance spectroscopy and chemometrics to predict soil organic carbon fractions. *Soil Tillage Res.* 85, 78–85. <https://doi.org/10.1016/j.still.2004.12.006>.
- Darvishi, Z., Morsali, A., 2011. Synthesis and characterization of Nano-bentonite by sonochemical method. *Ultrason. Sonochem.* 18, 238–242. <https://doi.org/10.1016/j.ulsonch.2010.05.012>.
- De Camillis, M., Di Emidio, G., Bezuijen, A., Verástegui-Flores, R.D., 2016. Hydraulic conductivity and swelling ability of a polymer modified bentonite subjected to wet-dry cycles in seawater. *Geotext. Geomembr.* 44 (5), 739–747. <https://doi.org/10.1016/j.geotextmem.2016.05.007>.
- Dehghani, Z., Ghaedi, M., Sabzehmeidani, M.M., Adhami, E., 2020. Removal of paraquat from aqueous solutions by a bentonite modified zero-valent iron adsorbent. *New J. Chem.* 44 (31), 13368–13376.
- Derudi, M., Venturini, G., Lombardi, G., Nano, G., Rota, R., 2007. Biodegradation combined with ozone for the remediation of contaminated soils. *Eur. J. Soil Biol.* 43, 265–272. <https://doi.org/10.1016/j.ejsobi.2007.03.001>.
- Diouri, K., Chaqroune, A., Kherbeche, A., Miyah, Y., Lahrichi, A., 2019. *International Journal of Innovative Research in Science. Eng. Technol.* 3, 16626–16637.
- Duman, O., Tunç, S., 2009. Electrokinetic and rheological properties of Na-bentonite in some electrolyte solutions. *Microporous Mesoporous Mater.* 117, 331–338. <https://doi.org/10.1016/j.micromeso.2008.07.007>.
- Elhadi, M., Samira, A., Mohamed, T., Djawad, F., Asma, A., Djamel, N., 2020. Removal of Basic Red 46 dye from aqueous solution by adsorption and photocatalysis: equilibrium, isotherms, kinetics, and thermodynamic studies. *Sep. Sci. Technol.* 55 (5), 867–885. <https://doi.org/10.1080/01496395.2019.1577896>.
- El-Sayed, G.O., Mohammed, T.Y., Salama, A.A.A., 2013. Batch adsorption of Maxilon red GRL from aqueous solution by natural sugarcane stalks powder. *ISRN Environ. Chem.* 2, 1–8. <https://doi.org/10.1155/2013/514154>.
- Fan, J., Guo, Y., Wang, J., Fan, M., 2009. Rapid decolorization of azo dye methyl orange in aqueous solution by nanoscale zerovalent iron particles. *J Hazard Mater.* 166, 904–910. <https://doi.org/10.1016/j.jhazmat.2008.11.091>.
- Farahmandjou, M., Soflae, F., 2015. Synthesis and characterization of α -Fe₂O₃ nanoparticles by simple co-precipitation method. *Phys. Chem. Res.* 3, 191–196. <https://doi.org/10.22036/PCR.2015.9193>.
- Gheraout, D., Gheraout, B., Kellil, A., 2009. Natural organic matter removal and enhanced coagulation as a link between coagulation and electrocoagulation. *Desalin. Water Treat.* 2, 203–222. <https://doi.org/10.5004/dwt.2009.116>.
- Ho, Y.S., Porter, J.F., McKay, G., 2002. Equilibrium isotherm studies for the sorption of divalent metal ions onto peat: copper, nickel and lead single component systems. *Water Air Soil Pollut.* 141, 1–33. <https://doi.org/10.1023/A:1021304828010>.
- Jana, S., Ray, J., Mondal, B., Tripathy, T., 2019. Efficient and selective removal of cationic organic dyes from their aqueous solutions by a nanocomposite hydrogel, katira gum-cl-poly(acrylic acid-co-N, N-dimethylacrylamide)@bentonite. *Appl. Clay Sci.* 173, 46–64. <https://doi.org/10.1016/j.clay.2019.03.009>.
- Karam, A., Zaher, K., Mahmoud, A.S., 2020. Comparative studies of using nano zerovalent iron, activated carbon, and green synthesized nano zerovalent iron for textile wastewater color removal using artificial intelligence, regression analysis, adsorption isotherm, and kinetic studies. *Air, Soil Water Res.* 13, 1–13. <https://doi.org/10.1177/1178622120908273>.
- Kelessidis, V.C., Tsamantaki, C., Dalamarinis, P., 2007. Effect of pH and electrolyte on the rheology of aqueous Wyoming bentonite dispersions. *Appl. Clay Sci.* 38, 86–96. <https://doi.org/10.1016/j.clay.2007.01.011>.
- Khan, M.R., Hegde, R.A., Shabiiam, M.A., 2017. Adsorption of lead by bentonite clay. *Int. J. Scientific Res. Manage.* 5 (7), 5800–5804 <http://resjournal.kku.ac.th>.
- Khodaer, E.A., 2015. Removal of Direct 50 dyes from aqueous solution using natural clay and organoclay adsorbents. *Baghdad Sci. J.* 12 (1), 157–166. <https://doi.org/10.21123/bsj.12.1.157-166>.
- Khrishieh, M.A.M., Al-Ghouti, M.A., Allen, S.J., Ahmad, M.N.M., 2004. The effect of pH, temperature, and molecular size on the removal of dyes from textile effluent using manganese oxides-modified diatomite. *Water Environ. Res. Water Environ. Res.* 76 (7), 2655–2663. <https://doi.org/10.1002/j.1554-7531.2004.tb00227.x>.
- Konicki, W., Aleksandrak, M., Mijowska, E., 2017. Equilibrium, kinetic and thermodynamic studies on adsorption of cationic dyes from aqueous solutions using graphene oxide. *Chem. Eng. Res. Des.* 123, 35–49. <https://doi.org/10.1016/j.cherd.2017.03.036>.
- Koyuncu, M., 2009. Removal of Maxilon Red GRL from aqueous solutions by adsorption onto silica. *Orient. J. Chem.* 25 (1), 35–40.
- Kundu, S., Gupta, A.K., 2006. Arsenic adsorption onto iron oxide-coated cement (IOCC): Regression analysis of equilibrium data with several isotherm models and their optimization. *Chem. Eng. J.* 122 (1–2), 93–106. <https://doi.org/10.1016/j.cej.2006.06.002>.
- Mahmoud, A.S., Farag, R.S., Elshfai, M.M., Mohamed, L.A., Ragheb, S.M., 2019. Nano Zero-Valent Aluminum (nZVAL) preparation, characterization, and application for the removal of soluble organic matter with artificial intelligence, isotherm study, and kinetic analysis. *Air, Soil Water Res.* 12. <https://doi.org/10.1177/1178622119878707>.
- Mahmoud, A.S., Mostafa, M.K., Abdel-gawad, S.A., 2018. Artificial intelligence for the removal of benzene, toluene, ethyl benzene and xylene (BTEX) from aqueous solutions using iron nanoparticles. *Water Supply.* 18, 1650–1663. <https://doi.org/10.2166/ws.2017.225>.
- Mahmoud, A.S., Farag, R.S., Elshfai, M.M., 2020. Reduction of organic matter from municipal wastewater at low cost using green synthesis nano iron extracted from black tea: artificial intelligence with regression analysis. *Egypt. J. Pet.* 29, 9–20. <https://doi.org/10.1016/j.ejpe.2019.09.001>.
- Martin, M.J., Artola, A., Balaguer, M.D., Rigola, M., 2003. Activated carbons developed from surplus sewage sludge for the removal of dyes from dilute aqueous solutions. *Chem. Eng. J.* 94 (3), 231–239. [https://doi.org/10.1016/S1385-8947\(03\)00054-8](https://doi.org/10.1016/S1385-8947(03)00054-8).
- Mo, J.H., Lee, Y.H., Kim, J., Jeong, J.Y., Jegal, J., 2008. Treatment of dye aqueous solutions using nanofiltration polyamide composite membranes for the dye wastewater reuse. *Dyes Pigm.* 76, 429–434. <https://doi.org/10.1016/j.dyepig.2006.09.007>.

- Mukhopadhyay, R., Adhikari, T., Sarkar, B., Barman, A., Paul, R., Patra, A.K., Sharma, P.C., Kumar, P., 2019. Adsorption of reactive dyes from aqueous solution by dirty bentonite. *Appl. Clay Sci. J. Hazard. Mater.* 376, 141–152. <https://doi.org/10.1016/j.jhazmat.2019.05.025>.
- Önal, M., Sarikaya, Y., 2007. Preparation and characterization of acidactivated bentonite powders. *Powder Technol.* 172, 14. <https://doi.org/10.1016/j.powtec.2006.10.034>.
- Pacula, A., Bielańska, E., Gawel, A., Bahranowski, K., Serwicka, E. M., 2006. Textural effects in powdered montmorillonite induced by freeze-drying and ultrasound pretreatment. *Appl. Clay Sci.* 32, 64–72. <https://doi.org/10.1016/j.clay.2005.10.002>.
- Sadaf, S., Bhatti, H.N., Nausheen, S., Amin, M., 2015. Application of a novel lignocellulosic biomaterial for the removal of Direct Yellow 50 dye from aqueous solution: batch and column study. *J. Taiwan Inst. Chem. Eng.* 47, 160–170. <https://doi.org/10.1016/j.jtice.2014.10.001>.
- Sheshdeh, R.K., Nikou, M.R.K., Badii, K., Limaee, N.Y., Golkarnarenji, G., 2014. Equilibrium and kinetics studies for the adsorption of Basic Red 46 on nickel oxide nanoparticles-modified diatomite in aqueous solutions. *J. Taiwan Inst. Chem. Eng.* 45 (4), 1792–1802. <https://doi.org/10.1016/j.jtice.2014.02.020>.
- Tohdee, K., Kaewsichan, L., 2018. Enhancement of adsorption efficiency of heavy metal Cu (II) and Zn (II) onto cationic surfactant modified bentonite. *J. Environ. Chem. Eng.* 6 (2), 2821–2828. <https://doi.org/10.1016/j.jece.2018.04.030>.
- Van olphen, H., 1977. *Clay colloid chemistry*. Interscience publishers, adivision of. John Wiley & Sons, New York.
- Wawrzkiwicz, M., Polska-adach, E., 2021. Physicochemical Interactions in Systems C.I. Direct Yellow 50 – Weakly Basic Resins: Kinetic, Equilibrium, and Auxiliaries Addition Aspects. *Water* 13, 385–404. <https://doi.org/10.3390/w13030385>.
- Wawrzkiwicz, M., Polska-Adach, E., Hubicki, Z., 2020. Polacrylic and polystyrene functionalized resins for direct dye removal from textile effluents. *Sep. Sci. Technol.* 55 (12), 2122–2136. <https://doi.org/10.1080/01496395.2019.1583254>.
- Wu, F.C., Tseng, R.L., Huang, S.C., Juang, R.S., 2009. Characteristics of pseudo-second-order kinetic model for liquid-phase adsorption: A mini-review. *Chem. Eng. J.* 151 (1–3), 1–9. <https://doi.org/10.1016/j.cej.2009.02.024>.
- Zhao, F., Rahunen, N., Varcoe, J.R., Roberts, A.J., Avignone-rossa, C., Thumser, A.E., Slade, R.C., 2009. Factors affecting the performance of microbial fuel cells for sulfur pollutants removal. *Biosens. Bioelectron.* 24, 1931–1936. <https://doi.org/10.1016/j.bios.2008.09.030>.